forests

MDPI

Article

Effects of Slope Position on the Rhizosphere and Fine Root Microbiomes of *Cupressus gigantea* on the Tibet Plateau, China

Wenfeng Gong [1], Liping Wei [2,*] and Jinliang Liu [3]

[1] College of Plant Science, Tibet Agricultural and Animal Husbandry University, Linzhi 860000, China; zkxygwf@xza.edu.cn
[2] Department of Resource and Environment, Tibet Agricultural and Animal Husbandry University, Linzhi 860000, China
[3] Key Laboratory of Silviculture on the Loess Plateau State Forestry Administration, College of Forestry, Northwest A&F University, Xianyang 712100, China; liujinliang2016@nwafu.edu.cn
* Correspondence: wlp20081013@xza.edu.cn

Abstract: *Cupressus gigantea* is an endangered species mainly distributed on beach land, down-slope, and middle-slope positions along the Yarlung Zangbo River on the Tibet Plateau of China, with an altitude ranging from 3000 to 3400 m. We investigated the rhizosphere and fine root microbiomes of *C. gigantea* at these three slope positions through metagenomic analysis. Slope positions had a greater influence on microbiome composition in the rhizosphere than that in the fine roots. Down- and middle-slope positions presented higher microbial richness indeces and community similarity, while a more complex co-occurrence network was observed in the beach land samples. Rhizosphere bacterial community assembly was determined via deterministic processes in the beach land and via stochastic processes in the down- and middle-slope positions. Archaeal and fungal community assemblies were both dominated by stochastic processes in the rhizosphere and fine roots at the three slope positions. Nitrogen (N) functional genes were more sensitive to changes in slope positions than phosphorus (N) functional genes. Soil properties explained more than 60% and 34% of the variations in the N and P functional genes and more than 30% and 10% of the variations in the microbiomes in the rhizosphere and fine roots, respectively. Variation in the microbiome was significantly driven by total nirtogen, total potassium, pH, and soil moisture in rhizosphere, and by pH and soil moisture in fine roots. Our observations suggest that the effect of slope position on the microbiomes of *C. gigantea* was greater for the rhizosphere than the fine roots, with down- and middle-slope positions presenting higher community similarity.

Keywords: slope position; rhizosphere microbiome; fine root microbiome; *C. gigantea*

Citation: Gong, W.; Wei, L.; Liu, J. Effects of Slope Position on the Rhizosphere and Fine Root Microbiomes of *Cupressus gigantea* on the Tibet Plateau, China. *Forests* **2024**, *15*, 897. https://doi.org/10.3390/f15060897

Academic Editor: Zuomin Shi

Received: 23 April 2024
Revised: 13 May 2024
Accepted: 20 May 2024
Published: 22 May 2024

1. Introduction

C. gigantea is an endangered species that is mainly distributed on the beach land, down-slope, and middle-slope along the Yarlung Zangbo River on the Tibet Plateau of China, with altitude ranging from 3000 to 3400 m [1]. The diameter at breast height (DBH) of *C. gigantea* ranges from 1 to 3 m, its height ranges from 30 to 45 m, and it can be used as an afforestation tree in the lower reaches of the Yarlung Zangbo River. *C. gigantea* plays an important role in biodiversity protection and ecological stability in the Yarlung Zangbo River. A variety of studies have reported the environmental suitability of *C. gigantea* [2,3], but knowledge on its rhizosphere and fine root microbiomes under different slope positions remains extremely limited.

The rhizosphere is a narrow zone of soil affected by root exudates, which can contain a huge number of microbes [4]. Root exudates are low-molecular-weight compounds that can shape the rhizosphere microbiome by changing the rhizosphere microenvironment, providing a nutrient source, and acting as signals [5,6]. Rhizosphere microbiomes play crucial roles in plant health and nutrient cycling in the rhizosphere [7] and are mainly

determined by the plant species, genotype, and development [8,9]. Furthermore, a variety of studies have reported that interactions between root exudates and soil properties regulate the rhizosphere microbiome [5,6,10,11].

The root microbiome comprises the microbes which colonize the plant roots, including mutualists, pathogens, and commensals [12]. The complex plant-associated microbial community is regarded as the second genome of the plant and plays a key role in the transformation and translocation of nutrients, the mitigation of environmental stresses, and protection from plant pathogens [13–15]. Microbial root endophytes are part of the root microbiome, with some being shown to have a positive influence on plant growth [16]. Soil properties and the host plant co-regulate the composition, structure, and assembly of the root microbial community [10].

The spatial heterogeneity caused by slope position can affect soil properties, vegetation types, and plant growth [17]; for example, down-slope transport and soil deposition result in the differentiation of soil water and substrates at different slope positions [17–19]. Increasing evidence has signified the importance of slope position in the spatial distribution of soil microbial communities and plants [17]. The rhizosphere microbiomes and root can directly affect plant functional traits, and the complex interactions between plants and microorganisms are necessary for plants to adapt to environmental habitats [7,10,20]. However, the effects of slope position on the rhizosphere and root microbiomes remain unclear.

The rhizosphere and root microbiomes are crucial for plants to adapt to different habitats [7,16]. Therefore, analysis of the composition, structure, function, and assembly of the rhizosphere and root microbiome can help us to understand the survival strategies and mechanisms of plants in different habitats [9,14,20]. In the present study, we analyze the composition, diversity, co-occurrence network, similarity, and assembly of the rhizosphere and root microbial communities of *C. gigantea* in beach land, down-slope, and middle-slope samples. The aims of this study are to (i) explore the variations in composition, diversity, structure, and function of the rhizosphere and root microbiomes among the three slope positions and (ii) uncover the key drivers affecting the rhizosphere and root microbiomes.

2. Materials and Methods

2.1. Study Site and Sampling

The study area was located in Lang county (93°04′–93°14′ E, 28°59′–29°03′ N), which is on the northern foot of the Himalayas and in the middle reaches of the Brahmaputra in the Tibet Plateau, China. The climate in this region is warm and semi-humid, with a mean annual temperature of 11 °C and an annual precipitation of 350–600 mm. More than 90% of the precipitation falls during the night during June~September, and the annual evaporation is four times the precipitation. The elevation ranges from 3000 m to 3200 m. The hillside was divided into three equal parts from the ridge to the valley, where down-slope and middle-slope, respectively, refer to the lower and middle parts of the hillside. The rhizosphere and fine root samples of *C. gigantea* in beach land, down-slope, and middle-slope positions were collected during July of 2023. The DBH values were 84.18 ± 18.25 cm, 83.08 ± 25.54 cm, and 115 ± 26.53 cm in beach land, down-slope, and middle-slope samples, respectively, and the height of trees in the three slope positions showed no difference, with values in the 16~17 m range.

Rhizosphere and root samples for microbial metagenomic analysis were collected according to the process described by Zhong et al. [21]. In brief, rhizosphere and root samples were collected in the topsoil layer (0–20 cm) in four directions from the trees using a sterile stainless steel corer (10 cm in diameter). Five *C. gigantea* sites were established in each slope position, and a total of 20 soil cores from 5 trees were mixed into 1 soil sample for each site. Soil was manually shaken from the fine roots (diameter less than 2 mm), and the remaining fine roots were transported to the laboratory in liquid nitrogen. A total of 15 rhizosphere samples and 15 fine root samples were collected in the three slope positions. The rhizosphere attached to the root surface was cleaned using a sonication

protocol and centrifuged for removal of roots. The remaining fine roots and collected rhizosphere samples were stored at −80 °C until metagenomic analysis.

2.2. Analysis of Rhizosphere Soil Properties

Rhizosphere soil organic carbon (SOC) was measured using an Elementar Liqui TOC II analyzer (Elementar Analysensysteme GmBH, Hanau, Germany), with the inorganic carbon removed using hydrochloric acid. Total nitrogen (TN) was measured using a Foss Kjeltec 8400 analyzer unit (Kjeltec Analyzer Unit, Hoganas, Sweden). Soil nitrate (NO_3^-) and ammonium (NH_4^+) were analyzed using a Lachat Flow Analyzer (AutoAnalyzer3-AA3, Mequon, WI, USA). Soil TP and AP were analyzed according to the methods described by Sparks et al. [22]. Soil total potassium (TK) and available potassium (AK) were measured using the flame photometer method with molten NaOH and NH4OAc extraction, respectively. Soil pH was analyzed using a pH meter (Sartorius PB-10, Sartorius, Germany) with 1:2.5 soil/water suspensions. Soil moisture (SM) was determined through weighing after drying in an oven (105 °C).

2.3. Microbial Metagenomic Sequencing

In brief, the total DNA in the rhizosphere and root were extracted using an E.Z.N.A.® Soil DNA Kit (Omega Bio-Tek, Doraville, GA, USA) based on the manufacturer's instructions. The concentration, purity, and quality of extracted DNA were checked using TBS-380, NanoDrop2000, and 1% agarose gel. The extracted DNA were fragmented into an average size of about 350 bp using Covaris M220 (Gene Company Limited, Beijing, China). The paired-end library was constructed using NEXTflex™ Rapid DNA-Seq (Bioo Scientific, Austin, TX, USA) and then performed on Illumina NovaSeq/Hiseq Xten (Illumina Inc., San Diego, CA, USA) by Majorbio Bio-Pharm Technology (Shanghai, China). The raw reads were cleaned by removing adaptor sequences and low-quality reads, and the optimized reads were assembled into contigs using MEGAHIT [23]. After the removal of contigs with length less than 300 bp, the remaining contigs were identified and clustered using MetaGene and CD-HIT, respectively [24]. Gene abundance in each sample was determined using SOAPaligner based on the non-redundant gene catalog with 95% identity [25]. Microbial taxonomic and KEGG information were annotated based on the NCBI NR database and the Kyoto Encyclopedia of Genes and Genomes database, respectively [26]. The accession number in NCBI is SRP507205.

2.4. Statistical Analysis

The variations in soil nutrients, microbial composition, diversity, normalized stochasticity ratio (NST), and function groups of N and P cycles among the three types were identified through one-way analysis of variance (ANOVA) and a least significant difference (LSD) multiple comparison test. Linear discriminant analysis effect size (LEfSe) analysis of microbes was conducted using the "microeco" package [27]. The similarity of rhizosphere and root microbial community compositions was analyzed through hierarchical cluster analysis using the "factoextra" package [28]. Microbial species with relative abundance greater than 0.01% in the rhizosphere and root were selected for co-occurrence network analysis, which was performed using the "igraph" package based on Pearson's correlation coefficients ($p < 0.05$, $r \geq 0.9$), after which visualization was performed with Gephi-0.9.2 [29]. The NST ratios of bacterial, fungal, and archaeal communities were determined using the "NST" packages [30]. The variations in N and P functional groups in the rhizosphere and root were analyzed through non-metric multi-dimensional scaling (NMDS) using the "vegan" package [31]. The effects of soil properties on bacterial, fungal, and archaeal community compositions and function groups were analyzed through redundancy analysis (RDA) using the "vegan" package [31]. The R software version used in this study was R v. 4.3.3.

3. Results

3.1. Rhizosphere Soil Properties

The values of SOC, TN, TP, TK, AP, and AK were significantly higher in middle-slope than in beach land and down-slope samples (Table 1). The NH_4^+ and NO_3^- contents showed no difference among the three slope positions. Soil stoichiometric ratio values increased with altitude, and the C:P and N:P ratios were significantly higher in middle-slope than that in beach land and down-slope samples. Lower pH and SM values were observed in the beach land samples.

Table 1. Rhizosphere soil properties of *C. gigantea* in three slope positions.

Soil Properties	Beach Land	Down-Slope	Middle-Slope	CV (%)	F	*p*
SOC (g kg^{-1})	2.77 ± 0.38 b	3.01 ± 1.12 b	6.58 ± 0.78 a	47.55	33.79	<0.001
TN (g kg^{-1})	0.24 ± 0.02 b	0.26 ± 0.09 b	0.56 ± 0.07 a	15.73	40.75	<0.001
TP (g kg^{-1})	0.50 ± 0.03 c	0.43 ± 0.04 b	0.57 ± 0.04 a	13.7	15.72	<0.001
TK (g kg^{-1})	8.42 ± 0.54 b	6.65 ± 0.42 c	10.43 ± 1.27 a	20.85	25.71	<0.001
NH_4^+ (mg kg^{-1})	2.88 ± 0.71	2.77 ± 0.8	3.48 ± 0.97	27.55	1.05	0.381
NO_3^- (mg kg^{-1})	22.63 ± 3.67	19.98 ± 0.69	19.49 ± 2.69	13.75	2.03	0.174
AP (mg kg^{-1})	7.08 ± 1.15 b	7.17 ± 1.56 b	10.12 ± 2.69 a	25.95	5.53	0.02
AK (mg kg^{-1})	59.66 ± 3.71 b	67.83 ± 15.63 b	212.29 ± 128.53 a	88.56	6.59	0.012
C:N	11.37 ± 1.22	11.45 ± 1.25	11.69 ± 0.16	8.24	0.13	0.876
C:P	5.56 ± 0.88 b	6.97 ± 2.46 b	11.63 ± 1.86 a	39.57	14.658	0.001
N:P	0.49 ± 0.05 b	0.60 ± 0.18 b	0.99 ± 0.16 a	37.39	17.55	<0.001
pH	8.29 ± 0.07 b	8.69 ± 0.23 a	8.77 ± 0.06 a	2.94	15.66	<0.001
SM (%)	3.74 ± 0.72 b	6.34 ± 1.21 a	4.54 ± 0.22 b	27.89	13.08	0.001
Altitude (m)	3010	3090	3220	-	-	-

Values are mean ± standard deviation (n = 5). Organic-carbon-to-total-nitrogen ratio (C:N); organic-carbon-to-phosphorus ratio (C:P); nitrogen-to-phosphorus ratio (N:P); CV: coefficient of variation. Different letters indicate significant differences ($p < 0.05$) in the same line based on one-way ANOVA followed by an LSD test.

3.2. Microbial Community Composition and Diversity

After quality filtering and assembly, the high-quality sequences were clustered into kingdoms of archaea, bacteria, and fungi. The archaeal community composition was dominated by Thaumarchaeota in the rhizosphere and by Euryarchaeota and Thaumarchaeota in fine roots. In the rhizosphere, the archaeal phyla of Thaumarchaeota, Euryarchaeota, Candidatus_Thermoplasmatota, Candidatus_Bathyarchaeota, and Candidatus_Woesearchaeota dominated, showing significant differences among the three sample types (Figure 1a). The relative abundance of Thaumarchaeota increased with altitude, with the highest value of 91.97% in middle-slope samples. In contrast, the relative abundance of other dominant archaeal phyla significantly decreased with altitude. In the fine roots, the relative abundances of Thaumarchaeota and Candidatus_thorarchaeota significantly increased and decreased with altitude, respectively (Figure 1b).

The bacterial community compositions were dominated by Actinobacteria and Proteobacteria in both the rhizosphere and fine roots. In the rhizosphere, the relative abundances of Actinobacteria and Proteobacteria significantly differed among the three sample types and, respectively, increased and decreased with altitude (Figure 1a). The other major bacterial phyla showed significant differences among the three sample types, with higher relative abundance values in the down-slope samples. In the fine roots, the phyla Acidobacteria, Planctomycetota, Chloroflexi, and Firmicutes showed significant differences, with higher relative abundance values observed in the down-slope samples (Figure 1b).

The fungal community compositions were dominated by Ascomycota in both the rhizosphere and fine roots. In the rhizosphere, the relative abundances of Ascomycota and Basidiomycota were significantly lower and higher in beach land samples than in other samples, respectively. The relative abundance of Zoopagomycota increased with altitude (Figure 1a). In the fine roots, higher abundance values of Ascomycota, Blastociadiomycota, and Basidiomycota were observed in the down-slope, beach land, and middle-slope samples, respectively (Figure 1b).

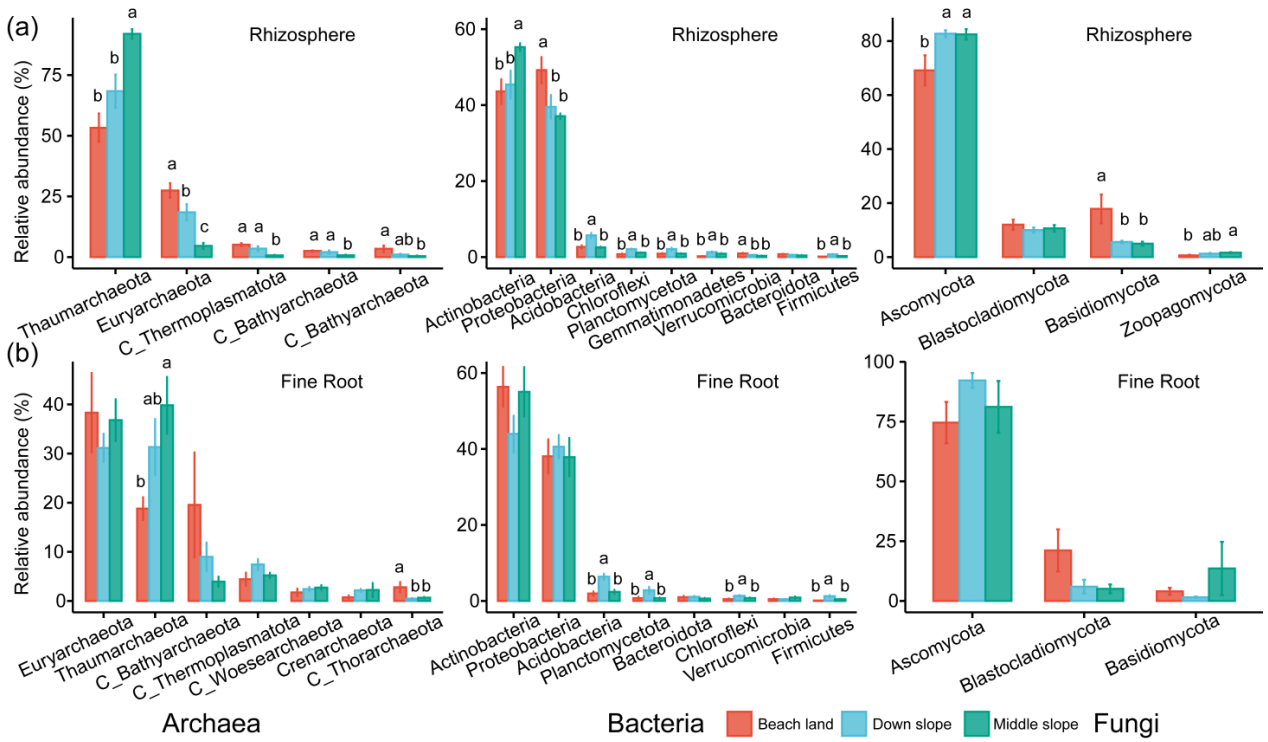

Figure 1. The compositions of archaeal, bacterial, and fungal communities at the phylum level in the rhizosphere soil (**a**) and fine roots (**b**). Different letters indicate a significant difference based on one-way ANOVA followed by an LSD test.

We analyzed the top 50 microbial genera in terms of abundance and found that microbial communities in down- and middle-slope positioins had a closer clustering distance in both rhizosphere and fine roots compared with beach land (Figure A1). About half of the microbial genera showed lower abundance values in beach land than in down- and middle-slope samples. Linear discriminant analysis effect size (LEfSe) analysis was conducted to identify the variation in species among the three slope positions, and the top 30 microbial clades based on the linear discriminant analysis (LDA) scores were listed (Figure A2). A total of 16 microbial clades were significantly enriched in the beach land rhizosphere, while 25 microbial clades were significantly enriched in the down-slope fine roots.

The Chao1 indices of archaeal, bacterial, and fungal communities significantly differed among three slope positions in the rhizosphere and fine roots, with lower values observed in the beach land samples (Figure 2a). The fungal Shannon–Wiener diversity value was lower in the beach land than in the down- and middle-slope samples in the rhizosphere and fine roots, but higher diversity values of archaeal and bacterial communities in fine root samples were observed for beach land (Figure 2b).

3.3. Microbial Community Similarity, Network and Assembly

Hierarchical cluster analysis was conducted to explore the similarity of microbial communities in the rhizosphere and fine roots between slope positions. In the rhizosphere, the similarities of archaeal, bacterial, and fungal communities revealed similar patterns, indicating that down- slope and middle-slope samples were clustered together, while the group of beach land samples was separately clustered (Figure 3a). In the fine roots, a similar clustering result was observed for the archaeal and bacterial communities, while the fungal groups of beach land and middle-slope samples had closer clustering distances (Figure 3b).

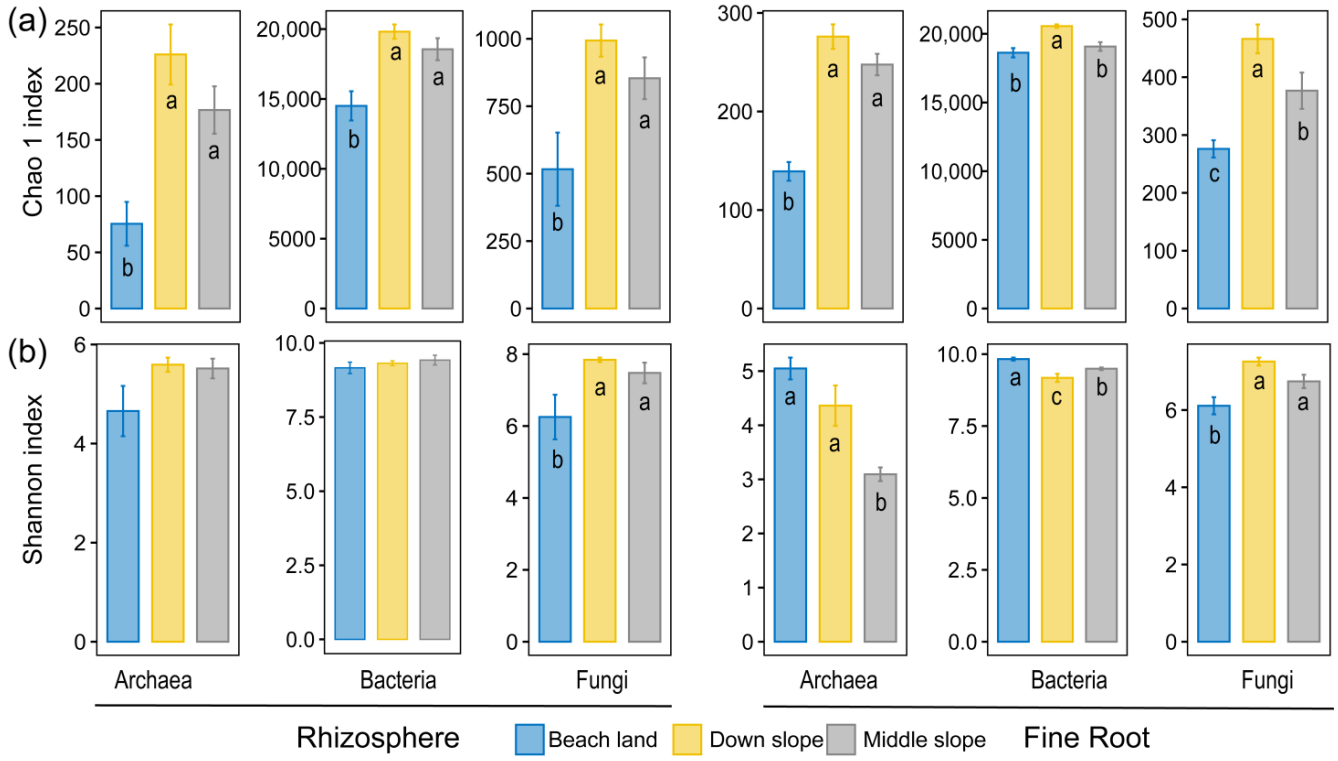

Figure 2. The Chao1 (**a**) and Shannon–Wiener (**b**) indices of archaeal, bacterial, and fungal communities at the species level in the rhizosphere and fine roots. Different letters indicate significant differences based on one-way ANOVA followed by an LSD test.

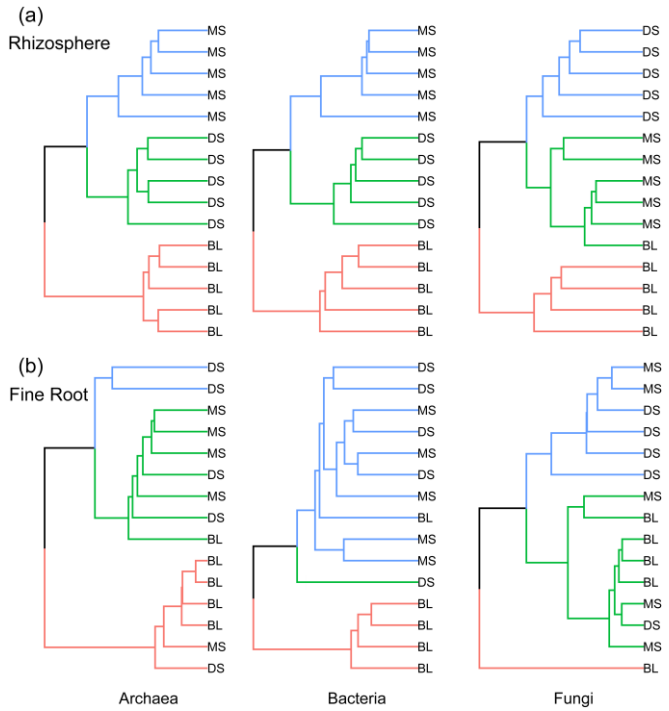

Figure 3. Hierarchical cluster analysis of archaeal, bacterial, and fungal communities at the species level in the rhizosphere (**a**) and fine roots (**b**). BL: beach land; DS: down-slope; MS: middle-slope.

Network topological metrics significantly differed among slope positions (Figure 4 and Table 2). A more complex root–rhizosphere microbial co-occurrence network was observed for the beach land samples, with the edge number being three times higher

than that for down-slope samples. The co-occurrence networks all showed a modular structure, with modularity values of >0.5 for the three slope positions of *C. gigantea*. The relationships among microorganisms in the co-occurrence networks were dominated by positive correlations, with the highest percentage of negative correlations observed in the down-slope samples (Table 2).

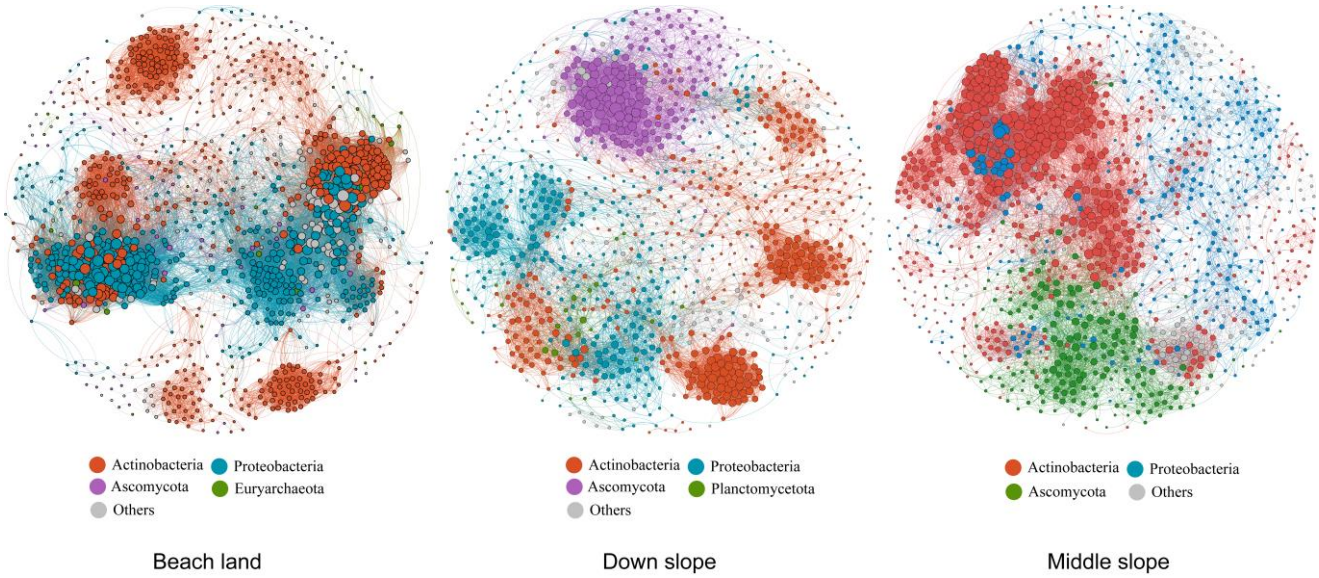

Figure 4. The microbial community networks at species level for three slope positions.

Table 2. Topological metrics of microbial community networks for three slope positions.

Network Properties	Beach Land	Down-Slope	Middle-Slope
Nodes	1239	1088	1182
Edges	37,296	11,701	14,131
Modules	34	28	34
Modularity	0.606	0.7	0.595
Transitivity	0.659	0.616	0.54
Density	0.05	0.019	0.02
Diameter	19.16	12.85	15.47
Positive correlation (%)	98.27	92.4	97.4
Negative correlation (%)	1.73	7.6	2.6

In the rhizosphere, the bacterial community assembly was dominated by deterministic processes (NST < 0.5) in the beach land samples and by stochastic processes (NST > 0.5) in the down-slope and middle-slope samples. The assemblies of archaeal and fungal communities were dominated by stochastic processes (NST > 0.5) in all three slope positions (Figure 5a). In the fine roots, the bacterial community assembly was dominated by deterministic processes (NST < 0.5) in the down-slope, while the assemblies of archaeal and fungal communities were dominated by stochastic processes (NST > 0.5) in all three slope positions (Figure 5b).

3.4. Microbial Community Functional Gene

N and P functional groups significantly differed among the slope positions in rhizosphere (stress = 0.061) and fine root (stress = 0.094) samples based on non-metric multidimensional scaling analysis (NMDS), as shown in Figure 6. The distance between points reflects the similarity of N and P functional genes, and down-slope and middle-slope samples had closer clustering distance in terms of both rhizosphere and fine roots. The majority of N functional genes significantly differed among slope positions for the rhizosphere (Table A1). Higher abundance values of nitrification genes were observed in middle-slope

samples, and higher abundance values of denitrification and nitrogen transport functional genes were observed in the beach land samples. Variations in N cycle genes were mainly dominated by denitrification genes, with higher abundance values in beach land than in down- and middle-slope fine root samples.

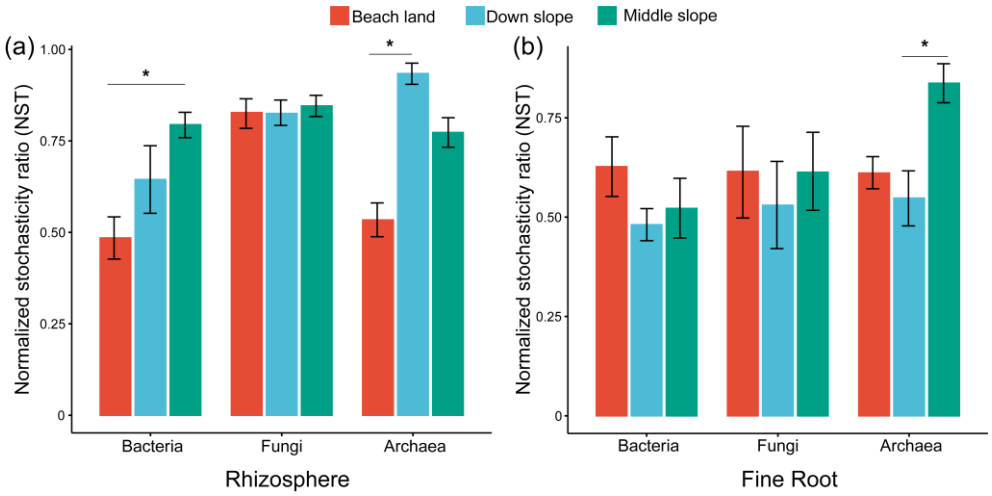

Figure 5. Microbial community assembly in the rhizosphere (**a**) and fine roots (**b**). The normalized stochasticity ratio (NST) was developed based on the Jaccard distance (NSTjac), with 0.5 as the boundary point between more deterministic (<0.5) and more stochastic (>0.5) community assemblies. * (p <0.05).

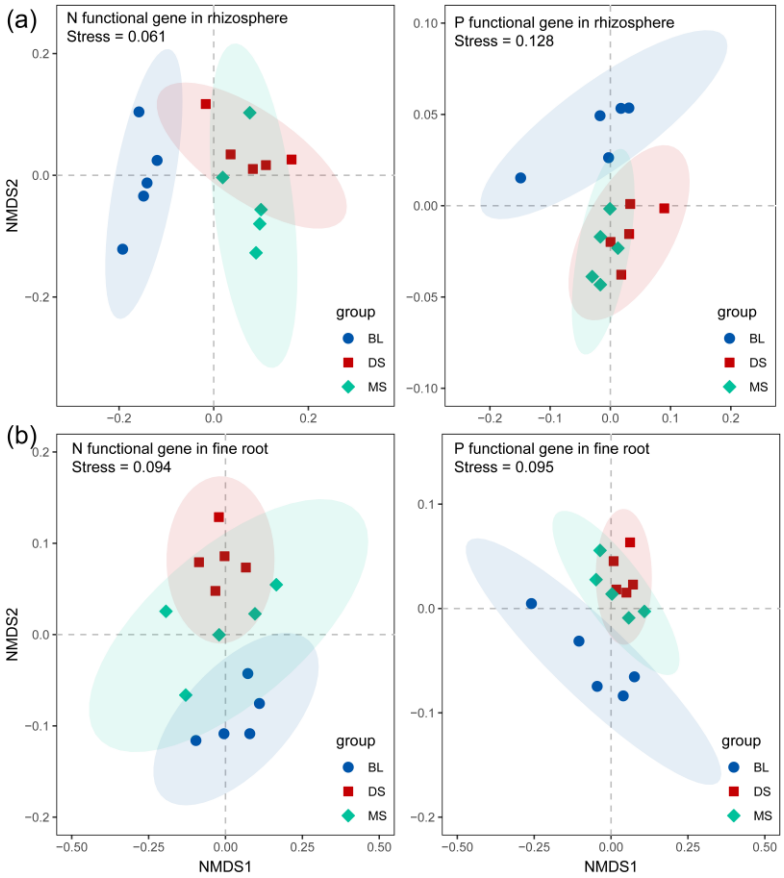

Figure 6. Non-metric multi-dimensional scaling analysis (NMDS) of N and P functional genes in the rhizosphere (**a**) and fine roots (**b**).

The majority of P functional genes showed no difference among the slope positions for both the rhizosphere and fine roots (Table A2). In the rhizosphere, variations in organic P mineralization were dominated by the genes phnX, phoD, 3-Phytase, and phnA, and their abundance values were higher in beach land than in down- and middle-slope samples. The functional genes of inorganic P solubilization significantly differed among slope positions, where higher abundance values were observed in the beach land samples. In the fine roots, organic P mineralization genes showed no difference among slope positions, while higher inorganic P solubilization genes were observed in the down-slope samples.

Soil properties explained 71.62% and 34.33% of the total variations in the N and P functional genes in the rhizosphere, respectively (Figure A1a). The first two RDA axes of N functional genes were significantly correlated with TK, N:P, pH, and soil moisture, and the first two RDA axes of P functional genes were significantly correlated with TK, C:N, N:P, pH, and soil moisture. Soil properties explained 61.08% and 43.05% of the total variations in the N and P functional genes in the fine roots, respectively (Figure A1b). The first two RDA axes of N functional genes were significantly correlated with TK, AP, N:P, pH, and soil moisture, and the first two RDA axes of P functional genes were significantly correlated with C:N, pH, and soil moisture.

3.5. Effects of Soil Properties on Microbial Community Composition

Soil properties explained 49.49% and 20.69% of the total variations in the archaeal community compositions in the rhizosphere and fine roots, respectively (Figure 7a). The first two archaeal RDA axes were significantly correlated with TP, TK, NO_3^-, C:P, pH, and soil moisture in the rhizosphere and with C:N, C:P, and pH in the fine roots. Soil properties explained 55.27% and 31.85% of the total variations in the bacterial community compositions in the rhizosphere and fine roots, respectively (Figure 7b). The first two bacterial RDA axes were significantly correlated with TP, TK, AP, pH, and soil moisture in the rhizosphere and with TK, NO_3^-, AP, C:P, pH, and soil moisture in the fine roots. Soil properties explained 29.97% and 10.53% of the total variations in the fungal community compositions in the rhizosphere and fine roots, respectively (Figure 7c). The first two fungal RDA axes were significantly correlated with TP, TK, AP, C:P, pH, and SM in the rhizosphere and with pH and SM in the fine roots.

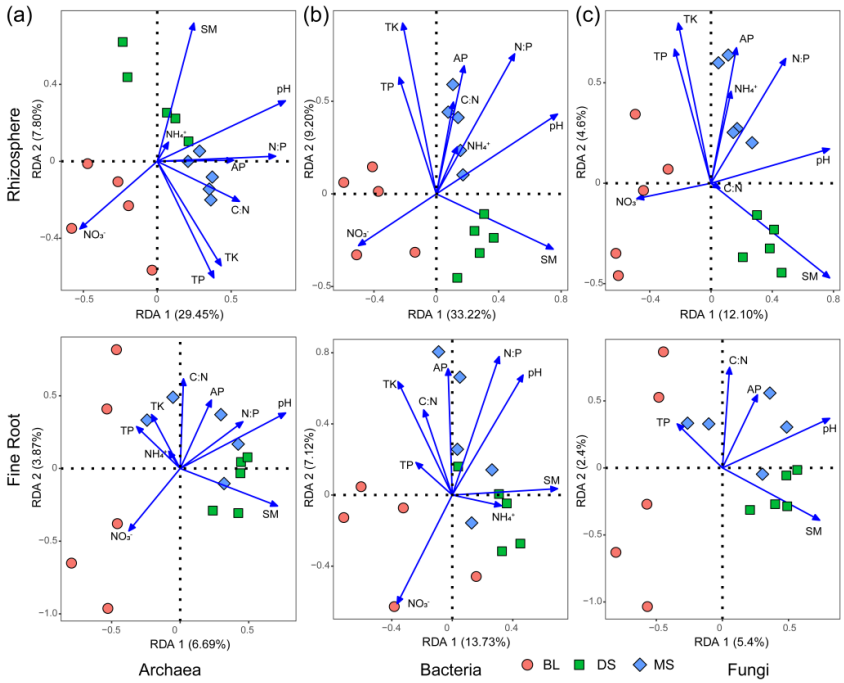

Figure 7. The effects of soil nutrients on archaeal (**a**), bacterial (**b**), and fungal (**c**) community compositions in the rhizosphere and fine roots.

4. Discussion

4.1. Microbial Community Composition and Diversity in Three Slope Positions

C. gigantea is an endangered species that plays a key role in preventing soil degradation and biodiversity protection along the Yarlung Zangbo River on the Tibet Plateau [2]. The distribution of *C. gigantea* is mainly in the beach land, down-slope, and middle-slope in sunny positions, and it is mainly distributed in the altitude range of 3000 m to 3400 m. The distribution characteristics of *C. gigantea* suggest that its survival has strict requirements regarding environmental factors. A variety of studies have reported the key roles of microorganisms in promoting plant growth, nutrient absorption, stress resistance, and disease resistance [32–34]. Therefore, microorganisms may play a key role in the survival of *C. gigantea*; however, knowledge of the microbial communities in the rhizosphere and fine roots of this species is poor. In the present study, we analyzed the composition, diversity, co-occurrence network, assemblies, functional groups of N and P cycles, and drivers of microbial communities in the rhizosphere and fine roots of *C. gigantea* across beach land, down-slope, and middle-slope positions.

Archaeal, bacterial, and fungal community compositions were more sensitive to changes in slope positions in the rhizosphere than in the fine roots [35]; for example, the dominant phyla significantly differed among slope positions in the rhizosphere, but only Thaumarchaeota revealed a significant difference in the fine roots. Actinobacteria are Gram-positive bacteria, which can produce secondary metabolites and work as symbionts and pathogens in plant–microbe interactions [36]. Most Actinobacteria are saprophytic and the relative abundance of Actinobacteria increased with slope position in this study, suggesting that more plant residues may accumulate in the down- and middle-slope positions [36]. Proteobacteria and Acidobacteria, respectively, belong to copiotrophic and oligotrophic groups, and the Proteobacteria–Acidobacteria ratio is positively associated with nutrient status [37]. The relative abundance of Proteobacteria decreased with slope position in the rhizosphere, and higher relative abundance values of Acidobacteria were observed in the down-slope compared with beach land and middle-slope positions, suggesting that the down-slope position may be characterized by lower nutrient status. This finding was confirmed by the observations of lower TP, TK, NH_4^+, and NO_3^- contents in the down-slope samples (Table 1). Furthermore, the relative abundances of Thaumarchaeota, Actinobacteria, and Ascomycota increased with slope position, suggesting that slope position may impose a differential pressure on the rhizosphere microbiome and selectively affect specific microbial groups [38].

In general, the Chao 1 richness index values of archaeal, bacterial, and fungal communities were significantly lower in beach land than in down- and middle-slope samples in the rhizosphere and fine roots. Combined with the finding that the down- and middle-slope microbiomes were clustered together, this suggests that the rhizosphere microbial communities were more similar between down- and middle-slope samples. Plants have a decisive effect on the rhizosphere microbiomes by the release of root exudates, and environmental factors also play key roles in regulating the microbial community compositions [39,40]. Considering that the nutrient status varied among slope positions, we suggest that environmental filtering may be the primary driver regulating community composition [41,42]. Furthermore, the fungal Shannon–Wiener diversity was lower in the beach land than in the down- and middle-slope rhizosphere and fine root samples, suggesting that changes in slope position increased the uncertainty of fungal community composition.

4.2. Microbial Community Network and Assembly

Microorganisms can form complex co-occurrence networks across niches, based on the cooperation of, and competition with, community members [13,41,43]. A more complex co-occurrence network was observed in the beach land samples, which was dominated by bacteria of the phyla of Actinobacteria and Proteobacteria, suggesting that close interaction between plants and bacteria is fundamental for understanding the survival strategies of *C. gigantea* in the beach land position [44,45]. The connections among microorganisms de-

creased in the co-occurrence networks of down- and middle-slope samples, with lower edge numbers, and the fungi of phylum of Ascomycota played a key role in the co-occurrence networks. The soil bacterial network is less stable than the fungal network under environmental stress, which can destabilize the microbial network [39,46]. The increase in the proportion of fungi in the microbial networks may improve network stability in the down- and middle-slope positions [46].

Deterministic and stochastic ecological processes associated with selection, dispersal, diversification, and drift play a controlling role in shaping the microbial community structure, which were used to describe the community assembly [47–49]. A normalized stochasticity ratio was developed based on the Jaccard distance to describe the deterministic (NST < 0.5) and stochastic (NST > 0.5) processes of microbial community assembly [30]. The rhizosphere bacterial community assembly shifted from being dominated by deterministic processes in the beach land samples to being dominated by stochastic processes in the down- and middle-slope samples, suggesting that the selection effect decreased with increasing of slope position [50]. Although archaeal community assemblies were dominated by stochastic processes in all slope positions in both the rhizosphere and fine roots, the influence strength of the stochastic process on community assemblies significantly differed. The fine root bacterial community assembly was dominated by deterministic process in the down-slope samples, while the influence strength of stochastic processes on the archaeal community assemblies significantly differed between down- and middle-slope samples. These observations confirm that the microbial strategies of *C. gigantea* are adapted to the slope position and differ between in the rhizosphere and fine roots [51].

4.3. Effects of Soil Properties on Microbial Community Composition and Functional Groups

The abundance and structure of functional genes of N and P cycles can help to link microbial groups to soil properties and ecosystem processes [52–54]. The effect of slope position was greater on N functional genes than on P functional genes, indicating that a majority of N functional genes significantly differed in the rhizosphere samples (Tables A1 and A2). The variations in N functional genes in the fine roots were dominated by denitrification, and the majority of P functional genes showed no difference among the three slope positions. Soil properties, respectively, explained 71.62% and 61.08% of the total variations in N functional genes in the rhizosphere and fine roots, and the variations were mainly driven by TK, N:P, pH, and SM (Figure A3). Soil properties, respectively, explained 34.33% and 43.05% of the total variations in P functional genes in the rhizosphere and fine roots, where the variations were mainly driven by C:N, pH, and SM. Our observations support the view that environmental filtering by pH and soil moisture plays an important role in regulating microbial functional genes in the rhizosphere and fine roots [55,56].

Soil properties, respectively, explained more variation in the archaeal, bacterial, and fungal community compositions in the rhizosphere than in the fine roots. The variations in microbial community compositions were mainly driven by TP, TK, pH, and soil moisture in the rhizosphere, and these findings could be partly explained by environmental factors and microbial substrate preferences [11,16,57–59]. Environmental filtering associated with soil pH and SM and the rhizosphere microbial community together affect the fine root microbial community, which has been shown to positively influence plant growth and health [16,60–62].

5. Conclusions

The effects of slope position on archaeal, bacterial, and fungal community compositions were greater in the rhizosphere than in the fine roots of *C. gigantea*. Compared with beach land, down- and middle-slope samples had higher microbial richness indices and a closer clustering distance. A more complex co-occurrence network dominated by bacteria was observed in the beach land sample, while the contribution of fungi to the microbial co-occurrence network increased in the down- and middle-slope samples. The rhizosphere bacterial community assembly was determined via deterministic processes in

beach land, while microbial community assemblies in down- and middle-slope positions were determined via stochastic processes. The N functional genes were more sensitive to changes in slope position than the P functional genes in the rhizosphere. The variations in microbial community compositions and functional genes were significantly affected by soil pH and moisture in the rhizosphere and fine roots. Our observations lay the foundation for exploring plant microbe interactions associated with *C. gigantea.*

Author Contributions: W.G.: Conceptualization, Data curation, Formal analysis, Investigation, Methodology; J.L. and L.W.: Conceptualization, Funding acquisition, Methodology, Project administration, Supervision, and Writing. All authors have read and agreed to the published version of the manuscript.

Funding: This work was financially supported by Joint Research Fund of Northwest A&F University and Tibet Agricultural and Animal Husbandry University (XNLH2022-02).

Data Availability Statement: The data presented in this study are available on request from the corresponding author.

Conflicts of Interest: The authors declare no conflicts of interest.

Appendix A

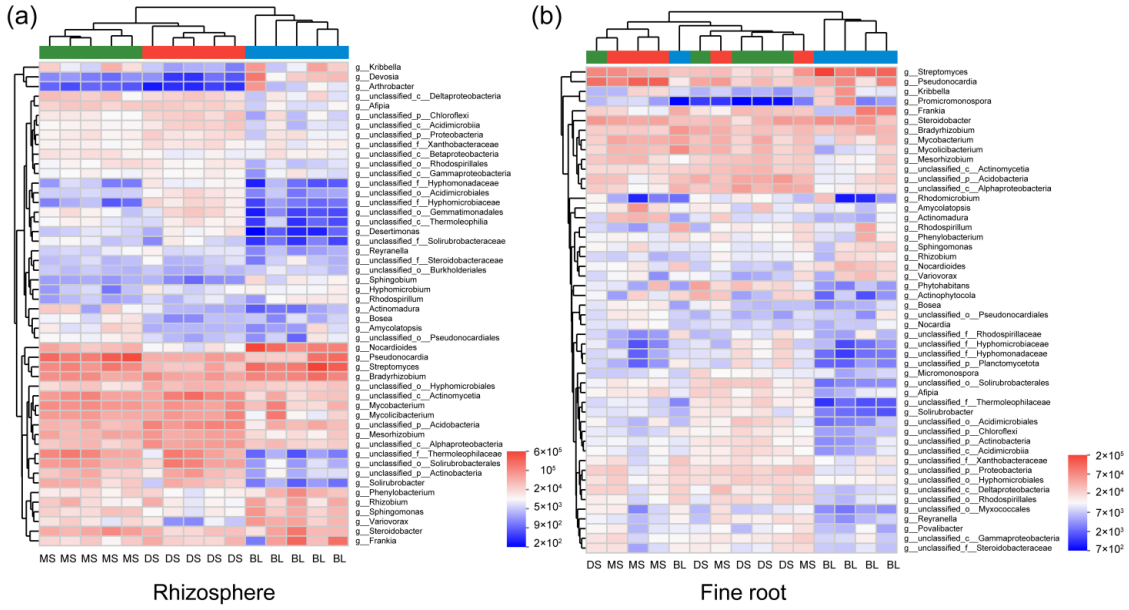

Figure A1. The abundances of the top 50 microbial genera in the rhizosphere (**a**) and fine roots (**b**) at three slope positions. The left and upper sides of the heat map show the species clustering tree and sample clustering tree, respectively. The red and blue colors represent the abundance of microbial species in the heat map.

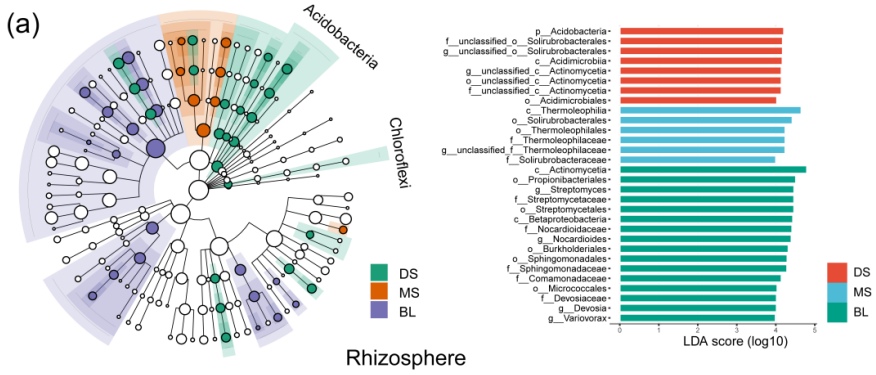

Figure A2. *Cont.*

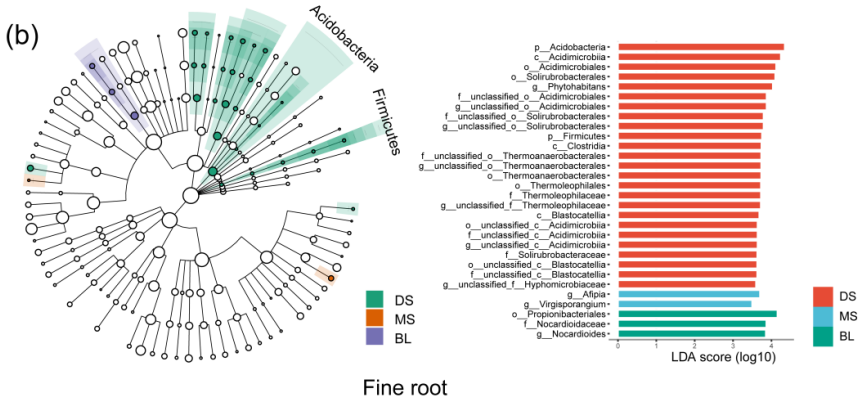

Figure A2. Linear discriminant analysis effect size (LEfSe) analysis of microbial abundance in the rhizosphere (**a**) and fine roots (**b**) among three slope positions. Linear discriminant analysis (LDA) score was used to identify the variation in species among the three slope positions.

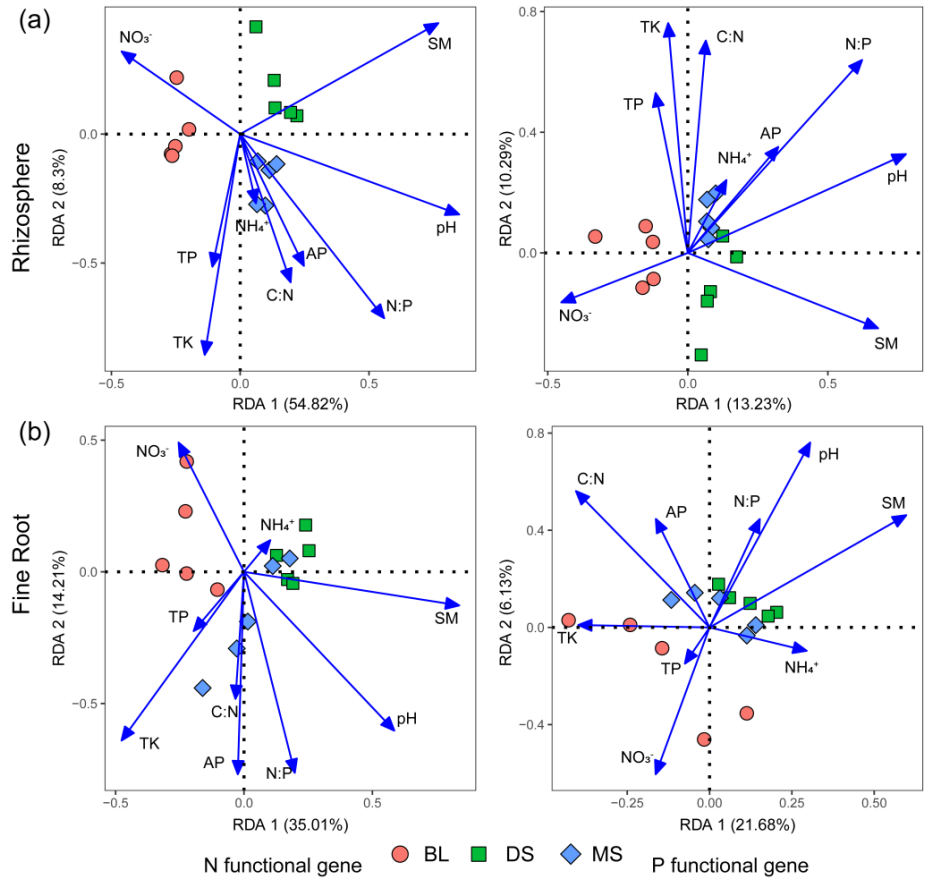

Figure A3. The effects of soil nutrients on N and P functional genes in the rhizosphere (**a**) and fine roots (**b**).

Table A1. Variations in N functional genes in the rhizosphere and fine roots among three slope positions.

Function	Gene	Rhizosphere				Fine Roots			
		Beach Land	Down-Slope	Middle-Slope	*p*	Beach Land	Down-Slope	Middle-Slope	*p*
Nitrogen fixation	nifD	10.17 ± 9.28	1.6 ± 1.13	4.05 ± 3.4	0.12	12.53 ± 12.03	2.36 ± 4.25	2.96 ± 3.57	0.124
	nifH	15.77 ± 13.42 a	0.95 ± 1.7 b	2.01 ± 2.27 b	0.021	19.26 ± 15.47 a	2.11 ± 2 b	1.42 ± 1.65 b	0.014
	nifK	12.79 ± 8.73 a	2.18 ± 1.29 b	5.63 ± 5.31 ab	0.046	9.71 ± 7.23	2.39 ± 4.17	1.94 ± 2.6	0.055
Nitrification	pmoA-moA	1.39 ± 1.06 b	3.24 ± 3.19 b	9.91 ± 4.84 a	0.005	1.72 ± 0.89	1.99 ± 1.35	1.39 ± 1.3	0.677
	pmoB-amoB	1.14 ± 1.28 b	5 ± 3.38 ab	8.59 ± 3.61 a	0.006	0.08 ± 0.18	1.92 ± 2.62	0.57 ± 0.41	0.188
	pmoC-amoC	2.09 ± 1.79 b	3.66 ± 1.43 b	9.16 ± 4.33 a	0.005	1.66 ± 2.21	1.26 ± 1.54	0.54 ± 0.8	0.556

Table A1. *Cont.*

Function	Gene	Rhizosphere				Fine Roots			
		Beach Land	Down-Slope	Middle-Slope	*p*	Beach Land	Down-Slope	Middle-Slope	*p*
Denitrification	nirK	77.67 ± 10.27 a	4.86 ± 3.04 b	7.37 ± 7.77 b	<0.001	48.94 ± 32.93 a	1.35 ± 1.35 b	1.9 ± 2.21 b	0.003
	norB	71.01 ± 19.4 a	1.89 ± 2.82 b	1.28 ± 1.14 b	<0.001	44.20 ± 34.04 a	3.57 ± 5.66 b	0.89 ± 1.37 b	0.008
	nosZ	25.63 ± 7.94 a	0.59 ± 1.18 b	1.41 ± 1.27 b	<0.001	26.72 ± 19.77 a	0.42 ± 0.76 b	0.69 ± 1.02 b	0.005
	narG/nxrA	261.43 ± 76.02 a	36.03 ± 6.74 b	77.95 ± 11.06 b	<0.001	181.14 ± 46.69 a	23.99 ± 12.68 b	82.61 ± 60.36 b	<0.001
	narH/nxrB	137.9 ± 42.47 a	18.35 ± 5.23 b	37.32 ± 6.8 b	<0.001	110.93 ± 21.58 a	13.84 ± 9.51 c	61.01 ± 39.96 b	<0.001
	narI	62.15 ± 22.96 a	8.3 ± 2.8 b	23.12 ± 8.55 b	<0.001	59.31 ± 30.08 a	5.81 ± 5.25 b	33.26 ± 21.54 ab	0.007
	napA	60.44 ± 8.33 a	17.42 ± 9.28 b	22.09 ± 12.12 b	<0.001	44.03 ± 27.91 a	19.72 ± 5.44 b	15.75 ± 6.08 b	0.042
	napB	14.15 ± 6.12 a	4.09 ± 3.42 b	5.11 ± 2.1 b	0.005	19.56 ± 21.88	1.84 ± 1.62	3.36 ± 2.27	0.089
	napC	18.28 ± 8.03 a	8.77 ± 9.17 ab	6.06 ± 1.84 b	0.045	17.4 ± 15.67	3.38 ± 1.36	5.97 ± 2.82	0.074
DNRA	nrfA	11.29 ± 5.03 a	9.02 ± 8.9 ab	1.64 ± 1.92 b	0.062	7.85 ± 7.46	12.98 ± 8.8	1.54 ± 1.56	0.058
	nrfH	7.63 ± 3.01 a	5.74 ± 4.36 a	0.53 ± 0.54 b	0.009	2.99 ± 3.95	4.32 ± 5.49	0.39 ± 0.88	0.312
	nirB	877.39 ± 124.35	738.18 ± 53.6	742.23 ± 90	0.061	639.62 ± 85.21	624.45 ± 79.41	694.44 ± 113.41	0.485
	nirD	216.79 ± 20.81 a	153.77 ± 19.76 c	192.13 ± 8.53 b	<0.001	180.75 ± 35.97	149.58 ± 25.69	202.6 ± 39.63	0.087
ANRA	nasA	574.95 ± 95.52 a	437.05 ± 58.24 b	412.6 ± 40.82 b	0.006	443.75 ± 45.85	438.16 ± 41.88	424.39 ± 110.36	0.911
	nasB	103.77 ± 15.14 a	25.49 ± 6.59 c	65.47 ± 15.43 b	<0.001	119.11 ± 31.84 a	50.12 ± 27.81 b	99.03 ± 47.88 ab	0.032
	narB	51.85 ± 19.5 b	94.65 ± 25.35 a	59.51 ± 12.09 b	0.011	31.99 ± 6.24	60.4 ± 17.26	54.7 ± 33.19	0.137
	nirA	80.84 ± 17.64	181.21 ± 16.1	159.92 ± 35.68	<0.001	62.32 ± 32.53	115.21 ± 26.67	98.5 ± 36.7	0.063
Nitrogen transport	NRT	485.42 ± 68.17 a	252.8 ± 32.9 b	299.69 ± 17.56 b	<0.001	365.33 ± 56.17 a	231.52 ± 23.24 c	288.96 ± 12.19 b	<0.001
	nrtA	339.4 ± 29.34 a	321.37 ± 40.27 a	258.01 ± 41.18 b	0.012	231.71 ± 64.86	231.59 ± 35.04	200.21 ± 85.86	0.688
	nrtB	229.4 ± 25.93 a	197.51 ± 34.68 ab	161.12 ± 23.86 b	0.009	152.88 ± 31.27	181.72 ± 33.89	139.27 ± 61.67	0.338
	nrtC	254.17 ± 21.62 a	210.8 ± 32.44 b	172.06 ± 17.78 c	0.001	170.02 ± 51.31	181.6 ± 22.06	147.66 ± 66.7	0.57
	nrtD	8.05 ± 6.98	11.87 ± 2.84	5.82 ± 2.48	0.151	8.16 ± 5.13	5.61 ± 4.07	8.41 ± 8.34	0.732
Organic N metabolism	gltB	1707.44 ± 192.92	1546.95 ± 64.21	1794.11 ± 213.12	0.106	1204.59 ± 135.51	996.35 ± 77.73	1117.9 ± 208.69	0.131
	gltD	591.74 ± 65.39 a	503.12 ± 48.65 b	595.08 ± 52.14 a	0.038	419.28 ± 33.14	352.67 ± 33.83	387.62 ± 69.56	0.138
	gdhA	164.47 ± 32.7 b	252.52 ± 73.46 a	244.84 ± 50.22 a	0.048	133.14 ± 23.54	133.96 ± 41.28	121.78 ± 37.91	0.831
	gdhB	44.3 ± 14.54 a	20.09 ± 4.34 b	27.24 ± 8.43 b	0.007	17.72 ± 9.87	15.8 ± 9.7	15.22 ± 11.12	0.922
	glnA	1758.66 ± 144.44 b	2130.77 ± 245.83 a	2317.58 ± 311.41 a	0.011	1446.07 ± 129.45	1437.17 ± 145.38	1449.5 ± 218.97	0.993
	ureB	105.35 ± 16.9 a	78.94 ± 9.68 b	82.26 ± 16.03 b	0.028	92.74 ± 15.11	81.24 ± 4.51	95.89 ± 8.14	0.098
	ureC	443.79 ± 47.76	433.77 ± 46.59	414.81 ± 41.56	0.604	341.23 ± 51.61	318.52 ± 31.74	357.28 ± 39.81	0.37
	ureA	108.36 ± 15.67 a	74.49 ± 13.15 b	79.99 ± 41.56 b	0.006	89.86 ± 35.4	70.82 ± 14.17	91.98 ± 23.97	0.395

Values are mean ± standard deviation (n = 5). Different letters in the same line indicate significant differences ($p < 0.05$) based on one-way ANOVA followed by an LSD test.

Table A2. Variation in P functional genes in the rhizosphere and fine roots among three slope positions.

Function	Gene	Rhizosphere				Fine Roots			
		Beach Land	Down-Slope	Middle-Slope	*p*	Beach Land	Down-Slope	Middle-Slope	*p*
Organic P mineralization	phnX	14.43 ± 2.25 b	28.46 ± 5.95 a	14.30 ± 2.39 b	<0.001	8.64 ± 7.08	26.26 ± 10.45	15.77 ± 7.88	0.22
	phnW	30.88 ± 5.35	44.77 ± 10.59	39.08 ± 9.19	0.07	35.18 ± 17.49	42.82 ± 17.33	28.81 ± 17.95	0.47
	phoA	123.24 ± 12.30	120.91 ± 10.63	113.24 ± 19.8	0.551	83.8 ± 31.1	108.86 ± 10.68	112.44 ± 16.64	0.17
	phoD	783.34 ± 48.75 b	913.92 ± 60.15 a	917.35 ± 30.93 a	0.001	774.09 ± 169.83	986.5 ± 56.74	891.93 ± 107.59	0.05
	appA	9.49 ± 8.8	6.39 ± 3.9	8.06 ± 4.01	0.814	6.36 ± 2.31	10.67 ± 10.15	6.58 ± 5.53	0.55
	3-Phytase	92.39 ± 16.14 b	124.16 ± 9.94 a	102.4 ± 7.01 ab	0.003	84.25 ± 54.89	121.19 ± 35.1	101.04 ± 19.97	0.36
	phnG	60.34 ± 24.97	62.87 ± 16.36	54.12 ± 3.07	0.72	44.88 ± 23.35	54.93 ± 9.45	52.81 ± 13.83	0.61
	phnH	69.32 ± 25.17	78.42 ± 13.94	64.85 ± 3.8	0.45	46.52 ± 16.04	51.14 ± 9.28	60.34 ± 12.21	0.26
	phnI	105.31 ± 31.99	130.39 ± 16.03	96.92 ± 7.19	0.067	73.54 ± 31.14	86.75 ± 15.63	97.31 ± 20.74	0.31
	phnJ	96 ± 25.7	87.85 ± 7.83	84.29 ± 4.94	0.505	61.54 ± 29.19	75.11 ± 13.44	68.81 ± 15.2	0.59
	phnL	57.38 ± 15.83	60.73 ± 7.57	57.39 ± 4.56	0.846	46.97 ± 14.42	50.41 ± 18.15	54.94 ± 9.23	0.69
	phnM	185.07 ± 32.6	176.29 ± 26.82	164.26 ± 18.07	0.482	139.71 ± 67.58	158.01 ± 11.4	149.97 ± 31.2	0.8
	phnN	61.89 ± 9.43	51.87 ± 14.63	45.86 ± 8.96	0.118	42.89 ± 26.23	39.45 ± 11.59	34.7 ± 2.82	0.74
	phnP	114.13 ± 23.88	119.72 ± 25.33	86.76 ± 10.46	0.062	80.37 ± 33.39	95.72 ± 30.39	63.47 ± 25.29	0.27
	phoN	5.29 ± 3.22	10.19 ± 1.21	10.39 ± 5.38	0.084	6.91 ± 5.76	14.16 ± 8.1	17.51 ± 12.45	0.22
Inorganic P solubilization	phnA	51.36 ± 13.71 b	82.32 ± 17.76 a	52.87 ± 10.57 b	0.008	47.37 ± 36	75.28 ± 19.11	51.96 ± 14.38	0.21
	gcd	346.92 ± 45.6 ab	407.7 ± 84.51 a	296.55 ± 35.82 b	0.036	258.28 ± 71.87 b	449.16 ± 103.22 a	350.29 ± 134.15 ab	0.05
	ppa	325.33 ± 45.55 a	226.46 ± 22.03 c	281.43 ± 13.78 b	0.001	297.11 ± 73.31 a	178.6 ± 30.06 b	197.61 ± 15.63 b	<0.001
	pqqC	96.38 ± 12.82 b	123.2 ± 12.49 a	128.18 ± 26.49 a	0.039	100.23 ± 29.36	113.79 ± 17.34	28.32 ± 32.81	0.3
	ppx-gppA	646.16 ± 92.16	637.49 ± 23.86	695.96 ± 43.69	0.293	505.14 ± 87.29	482.42 ± 38.19	514.87 ± 53.36	0.71
Regulatory	phoB	213.55 ± 48.24	207.97 ± 15.73	184.22 ± 31.94	0.392	121.43 ± 27.27 b	188.71 ± 36.17 a	132.38 ± 45.98 b	0.04
	phoR	402.89 ± 105.78 a	319.19 ± 26.59 ab	241.52 ± 21.77 b	0.006	239.8 ± 76.08	260.68 ± 32.08	237.99 ± 102.91	0.87
	phoP	26.36 ± 7.4 a	11.23 ± 2.69 b	13.88 ± 3.05 b	0.001	26.36 ± 14.96	12.87 ± 5.69	19.39 ± 13.91	0.26
	phoU	387.38 ± 26.87	421.83 ± 34.12	419.44 ± 33.43	0.2	326.16 ± 38.67 b	359.17 ± 18.46 ab	379.89 ± 18.29 a	0.03
Transporters	phnC	182.26 ± 22.76	202.09 ± 37.84	191.52 ± 22.33	0.563	163.98 ± 74.38	163.87 ± 26.55	205.06 ± 25.39	0.33
	phnD	214.51 ± 31.66 b	260.89 ± 18.06 a	228.06 ± 23.92 ab	0.035	182.03 ± 101.75	237.8 ± 34.64	229.9 ± 45.4	0.4
	phnE	279.45 ± 57.03	278.21 ± 26.64	240.46 ± 18.48	0.222	183.17 ± 70.63	261.36 ± 33.42	246.27 ± 45.20	0.08
	pstA	414.31 ± 52.41	411.78 ± 25.93	389.19 ± 25.4	0.513	333.16 ± 39.23	325.57 ± 31.44	302.53 ± 14.46	0.29
	pstB	518.14 ± 60.74	515.15 ± 62.33	484.78 ± 43.71	0.597	409.64 ± 39.56	371.37 ± 32.73	376.79 ± 60.53	0.39
	pstC	396.09 ± 41.68	434.83 ± 18.93	396.25 ± 19.31	0.086	349.22 ± 22.54	347. ± 24.8	329.64 ± 32.63	0.48
	pstS	698.02 ± 66.07 b	798.82 ± 23.6 a	824.09 ± 62.79 a	0.008	657.74 ± 159.74	734.2 ± 45.44	767.56 ± 60.61	0.26
	phnK	83.84 ± 23.69	71.78 ± 12.88	73.34 ± 8.96	0.472	59.15 ± 17.74	57.69 ± 16.58	60.67 ± 18.57	0.97
	phnF	71.27 ± 27.2	74.49 ± 9.14	66.94 ± 11.39	0.801	34.8 ± 20.4 b	76.79 ± 23.22 a	83.75 ± 24.78 a	0.01
	TC.PIT	322.54 ± 85.9 a	184.92 ± 15.85 b	270.37 ± 42.69 a	0.007	273.27 ± 85.64 a	134.17 ± 26.89 b	191.49 ± 38.52 b	0.01
	ugpA	184.13 ± 35.76	184.64 ± 15.03	192.96 ± 30.83	0.862	155.67 ± 24.31	170.96 ± 31.39	165.59 ± 43.69	0.78
	ugpB	274.65 ± 43.22	286.37 ± 29.88	305.17 ± 12.51	0.532	225.89 ± 70.24	246.74 ± 50.21	241.16 ± 23.92	0.81
	ugpC	188.35 ± 47.45	165.43 ± 19.8	159.91 ± 10.67	0.326	121.9 ± 47.61	114.35 ± 15.82	129.63 ± 26.75	0.77
	ugpE	204.35 ± 49.93	184.51 ± 6.9	184.39 ± 10.69	0.495	178.34 ± 49.23	172.87 ± 36.76	164.66 ± 14.18	0.84
	glpQ	848.43 ± 159.39	813.6 ± 97.79	872.57 ± 67.68	0.723	805.45 ± 208.68	734.25 ± 60.3	768.34 ± 52.83	0.69
Polyphosphate synthesis	ppk1	702.1 ± 56.68	747.3 ± 37.79	797.5 ± 75.07	0.071	488.24 ± 80.49	483.92 ± 48.61	535.44 ± 111.83	0.58
	ppaC	5.89 ± 2.62 b	23.03 ± 9.09 a	36.81 ± 15.02 a	0.002	3.99 ± 3.23 b	8.55 ± 6.46 b	17.58 ± 10.95 a	0.04
	ppk2	320.61 ± 19.55 a	257.3 ± 35.34 b	261.04 ± 30.53 b	0.008	313.67 ± 63.64	241.78 ± 20.4	259.42 ± 36.18	0.07
	surE	267.1 ± 34.64	280.96 ± 27.49	287.62 ± 23.95	0.536	190.2 ± 54.74	237.88 ± 33.88	219.14 ± 41.7	0.27
Polyphosphate degradation	pap	71.8 ± 17.02	90.63 ± 16.91	93.98 ± 13.57	0.099	61.06 ± 20.34	63.61 ± 18.75	61.43 ± 22.97	0.98
	ppnK	320.08 ± 14.15	341.23 ± 29.08	340.87 ± 48.02	0.537	267.19 ± 39.19	239.72 ± 23.82	254.62 ± 32.42	0.42
	ppgK	115.65 ± 17.12	103.21 ± 13.37	105.37 ± 11.2	0.362	123.86 ± 27.19	110.08 ± 25.43	116.59 ± 20.62	0.68
	relA	85.42 ± 18.7 a	42.06 ± 9.53 b	57.71 ± 7.93 b	0.001	58.55 ± 24.99	40.15 ± 17.38	52.16 ± 30.63	0.52
	spoT	858.36 ± 83.39	822.56 ± 86.08	839.47 ± 134.86	0.232	565.83 ± 98.02	509.28 ± 27.21	549.99 ± 103.88	0.56
	HDDC3	6.54 ± 5.33 b	16.64 ± 5.58 a	15.19 ± 3.57 a	0.022	8.35 ± 5.52 b	26.79 ± 7.88 a	22.85 ± 10.65 a	0.01
	ndk	237.22 ± 13.3 a	212.52 ± 18.32 b	215.21 ± 12.96 b	0.045	192.23 ± 31.85	158.7 ± 25.22	168.58 ± 21.68	0.17
	PK	558.14 ± 79.74	515.33 ± 49.06	528.97 ± 55.2	0.561	388.39 ± 44.43	346.33 ± 29.97	363.17 ± 65.12	0.42

Values are mean ± standard deviation (n = 5). Different letters in the same line indicate significant differences ($p < 0.05$) based on one-way ANOVA followed by an LSD test.

References

1. Raddi, P.; Della Rocca, G.; Danti, R. Cupressus Berendsen. In *Enzyklopädie der Holzgewächse: Handbuch und Atlas der Dendrologie*; John Wiley & Sons: Hoboken, NJ, USA, 2014; pp. 1–15. [CrossRef]
2. Lei, P.; Liu, Z.; Li, J.; Jin, G.; Xu, L.; Ji, X.; Zhao, X.; Tao, L.; Meng, F. Integration of the physiology, transcriptome and proteome reveals the molecular mechanism of drought tolerance in *Cupressus gigantea*. *Forests* **2022**, *13*, 401. [CrossRef]
3. Zhang, H.; Wei, Y.; Yue, J.; Wang, Z.; Zou, H.; Ji, X.; Zhang, S.; Liu, Z. Prediction of Potential Suitable Areas and Priority Protection for *Cupressus gigantea* on the Tibetan Plateau. *Plants* **2024**, *13*, 896. [CrossRef] [PubMed]
4. Philippot, L.; Raaijmakers, J.M.; Lemanceau, P.; Van Der Putten, W.H. Going back to the roots: The microbial ecology of the rhizosphere. *Nat. Rev. Microbiol.* **2013**, *11*, 789–799. [CrossRef]
5. Hartman, K.; Tringe, S.G. Interactions between plants and soil shaping the root microbiome under abiotic stress. *Biochem. J.* **2019**, *476*, 2705–2724. [CrossRef] [PubMed]
6. Koprivova, A.; Kopriva, S. Plant secondary metabolites altering root microbiome composition and function. *Curr. Opin. Plant Biol.* **2022**, *67*, 102227. [CrossRef] [PubMed]
7. Zechmeister-Boltenstern, S.; Keiblinger, K.M.; Mooshammer, M.; Peñuelas, J.; Richter, A.; Sardans, J.; Wanek, W. The application of ecological stoichiometry to plant-microbial-soil organic matter transformations. *Ecol. Monogr.* **2015**, *85*, 133–155. [CrossRef]
8. Chaparro, J.M.; Badri, D.V.; Vivanco, J.M. Rhizosphere microbiome assemblage is affected by plant development. *ISME J.* **2014**, *8*, 790–803. [CrossRef] [PubMed]
9. Tkacz, A.; Bestion, E.; Bo, Z.; Hortala, M.; Poole, P.S. Influence of plant fraction, soil, and plant species on microbiota: A multikingdom comparison. *MBio* **2020**, *11*, 10–1128. [CrossRef] [PubMed]
10. Berendsen, R.L.; Pieterse, C.M.; Bakker, P.A. The rhizosphere microbiome and plant health. *Trends Plant Sci.* **2012**, *17*, 478–486. [CrossRef]
11. Sasse, J.; Martinoia, E.; Northen, T. Feed your friends: Do plant exudates shape the root microbiome? *Trends Plant Sci.* **2018**, *23*, 25–41. [CrossRef]
12. Bai, B.; Liu, W.; Qiu, X.; Zhang, J.; Zhang, J.; Bai, Y. The root microbiome: Community assembly and its contributions to plant fitness. *J. Integr. Plant Biol.* **2022**, *64*, 230–243. [CrossRef] [PubMed]
13. Barberán, A.; Bates, S.T.; Casamayor, E.O.; Fierer, N. Using network analysis to explore co-occurrence patterns in soil microbial communities. *ISME J.* **2012**, *6*, 343–351. [CrossRef] [PubMed]
14. Lundberg, D.S.; Lebeis, S.L.; Paredes, S.H.; Yourstone, S.; Gehring, J.; Malfatti, S.; Tremblay, J.; Engelbrektson, A.; Kunin, V.; Del Rio, T.G.; et al. Defining the core Arabidopsis thaliana root microbiome. *Nature* **2012**, *488*, 86–90. [CrossRef] [PubMed]
15. Pascale, A.; Proietti, S.; Pantelides, I.S.; Stringlis, I.A. Modulation of the root microbiome by plant molecules: The basis for targeted disease suppression and plant growth promotion. *Front. Plant Sci.* **2020**, *10*, 501717. [CrossRef] [PubMed]
16. Gaiero, J.R.; McCall, C.A.; Thompson, K.A.; Day, N.J.; Best, A.S.; Dunfield, K.E. Inside the root microbiome: Bacterial root endophytes and plant growth promotion. *Am. J. Bot.* **2013**, *100*, 1738–1750. [CrossRef] [PubMed]
17. Bardelli, T.; Gómez-Brandón, M.; Ascher-Jenull, J.; Fornasier, F.; Arfaioli, P.; Francioli, D.; Pietramellara, G. Effects of slope exposure on soil physico-chemical and microbiological properties along an altitudinal climosequence in the Italian Alps. *Sci. Total Environ.* **2017**, *575*, 1041–1055. [CrossRef] [PubMed]
18. Huang, Y.M.; Liu, D.; An, S.S. Effects of slope aspect on soil nitrogen and microbial properties in the Chinese Loess region. *Catena* **2015**, *125*, 135–145. [CrossRef]
19. Sun, Q.; Hu, Y.; Wang, R.; Guo, S.; Yao, L.; Duan, P. Spatial distribution of microbial community composition along a steep slope plot of the Loess Plateau. *Appl. Soil. Ecol.* **2018**, *130*, 226–236. [CrossRef]
20. Zhang, R.; Vivanco, J.M.; Shen, Q. The unseen rhizosphere root-soil-microbe interactions for crop production. *Curr. Opin. Microbiol.* **2017**, *37*, 8–14. [CrossRef]
21. Zhong, Y.; Sorensen, P.O.; Zhu, G.; Jia, X.; Liu, J.; Shangguan, Z.; Yan, W. Differential microbial assembly processes and co-occurrence networks in the soil-root continuum along an environmental gradient. *IMETA* **2022**, *1*, e18. [CrossRef]
22. Sparks, D.L.; Page, A.L.; Helmke, P.A.; Loeppert, R.H. (Eds.) *Methods of Soil Analysis, Part 3: Chemical Methods*; John Wiley & Sons: Hoboken, NJ, USA, 2020; Volume 14.
23. Li, D.; Liu, C.M.; Luo, R.; Sadakane, K.; Lam, T.W. MEGAHIT: An ultra-fast single-node solution for large and complex metagenomics assembly via succinct de Bruijn graph. *Bioinformatics* **2015**, *31*, 1674–1676. [CrossRef] [PubMed]
24. Noguchi, H.; Park, J.; Takagi, T. MetaGene: Prokaryotic gene finding from environmental genome shotgun sequences. *Nucleic Acids Res.* **2006**, *34*, 5623–5630. [CrossRef]
25. Gu, S.; Fang, L.; Xu, X. Using SOAPaligner for short reads alignment. *Curr. Protoc. Bioinform.* **2013**, *44*, 11.11.1–11.11.17. [CrossRef] [PubMed]
26. Lavigne, R.; Seto, D.; Mahadevan, P.; Ackermann, H.W.; Kropinski, A.M. Unifying classical and molecular taxonomic classification: Analysis of the Podoviridae using BLASTP-based tools. *Res. Microbiol.* **2008**, *159*, 406–414. [CrossRef] [PubMed]
27. Liu, C.; Cui, Y.; Li, X.; Yao, M. microeco: An R package for data mining in microbial community ecology. *FEMS Microbiol. Ecol.* **2021**, *97*, fiaa255. [CrossRef] [PubMed]
28. Kassambara, A.; Mundt, F. Package 'Factoextra'. Extract and Visualize the Results of Multivariate Data Analyses. 2017, 76. Available online: https://piyanit.nl/wp-content/uploads/2020/10/factoextra.pdf (accessed on 1 January 2024).

29. Bastian, M.; Heymann, S.; Jacomy, M. Gephi: An open source software for exploring and manipulating networks. *Proc. Int. AAAI Conf. Web Soc. Media* **2009**, *3*, 361–362. [CrossRef]
30. Ning, D.; Deng, Y.; Tiedje, J.M.; Zhou, J. A general framework for quantitatively assessing ecological stochasticity. *PNAS* **2019**, *116*, 16892–16898. [CrossRef]
31. Oksanen, J.; Blanchet, F.G.; Kindt, R.; Legendre, P.; Minchin, P.R.; O'hara, R.B.; Solymos, P.; Stevens, M.H.H.; Szoecs, E.; Wagner, H.; et al. Package 'Vegan'. Community Ecology Package, Version. **2013**, *2*, 1–295. Available online: https://mirrors.aliyun.com/CRAN/web/packages/vegan/vegan.pdf (accessed on 1 January 2024).
32. Lemke, M.; DeSalle, R. The next generation of microbial ecology and its importance in environmental sustainability. *Microb. Ecol.* **2023**, *85*, 781–795. [CrossRef]
33. Finkel, O.M.; Salas-González, I.; Castrillo, G.; Conway, J.M.; Law, T.F.; Teixeira, P.J.P.L.; Wilson, E.D.; Fitzpatrick, C.R.; Jones, C.D.; Dangl, J.L. A single bacterial genus maintains root growth in a complex microbiome. *Nature* **2020**, *587*, 103–108. [CrossRef]
34. Trivedi, P.; Batista, B.D.; Bazany, K.E.; Singh, B.K. Plant-microbiome interactions under a changing world: Responses, consequences and perspectives. *New Phytol.* **2022**, *234*, 1951–1959. [CrossRef] [PubMed]
35. Gottel, N.R.; Castro, H.F.; Kerley, M.; Yang, Z.; Pelletier, D.A.; Podar, M.; Karpinets, T.; Uberbacher, E.; Tuskan, G.A.; Vilgalys, R.; et al. Distinct microbial communities within the endosphere and rhizosphere of Populus deltoides roots across contrasting soil types. *Appl. Environ. Microbiol.* **2011**, *77*, 5934–5944. [CrossRef] [PubMed]
36. Barka, E.A.; Vatsa, P.; Sanchez, L.; Gaveau-Vaillant, N.; Jacquard, C.; Klenk, H.P.; Clément, C.; Ouhdouch, Y.; van Wezel, G.P. Taxonomy, physiology, and natural products of Actinobacteria. *Microbiol. Mol. Biol. Rev.* **2016**, *80*, 1–43. [CrossRef] [PubMed]
37. Orwin, K.H.; Dickie, I.A.; Holdaway, R.; Wood, J.R. A comparison of the ability of PLFA and 16S rRNA gene metabarcoding to resolve soil community change and predict ecosystem functions. *Soil. Biol. Biochem.* **2018**, *117*, 27–35. [CrossRef]
38. Cui, Y.; Bing, H.; Fang, L.; Wu, Y.; Yu, J.; Shen, G.; Jiang, M.; Wang, X.; Zhang, X. Diversity patterns of the rhizosphere and bulk soil microbial communities along an altitudinal gradient in an alpine ecosystem of the eastern Tibetan Plateau. *Geoderma* **2019**, *338*, 118–127. [CrossRef]
39. Hernandez, D.J.; David, A.S.; Menges, E.S.; Searcy, C.A.; Afkhami, M.E. Environmental stress destabilizes microbial networks. *ISME J.* **2021**, *15*, 1722–1734. [CrossRef] [PubMed]
40. Li, C.; Jin, L.; Zhang, C.; Li, S.; Zhou, T.; Hua, Z.; Wang, L.; Ji, S.; Wang, Y.; Gan, Y.; et al. Destabilized microbial networks with distinct performances of abundant and rare biospheres in maintaining networks under increasing salinity stress. *IMeta* **2023**, *2*, e79. [CrossRef]
41. Jiao, S.; Yang, Y.; Xu, Y.; Zhang, J.; Lu, Y. Balance between community assembly processes mediates species coexistence in agricultural soil microbiomes across eastern China. *ISME J.* **2020**, *14*, 202–216. [CrossRef]
42. Liu, J.; Wang, Q.; Ku, Y.; Zhang, W.; Zhu, H.; Zhao, Z. Precipitation and soil pH drive the soil microbial spatial patterns in the Robinia pseudoacacia forests at the regional scale. *Catena* **2022**, *212*, 106120. [CrossRef]
43. Bauer, M.A.; Kainz, K.; Carmona-Gutierrez, D.; Madeo, F. Microbial wars: Competition in ecological niches and within the microbiome. *Microb. Cell* **2018**, *5*, 215. [CrossRef]
44. Bulgarelli, D.; Schlaeppi, K.; Spaepen, S.; Van Themaat, E.V.L.; Schulze-Lefert, P. Structure and functions of the bacterial microbiota of plants. *Annu. Rev. Plant Biol.* **2013**, *64*, 807–838. [CrossRef] [PubMed]
45. Wagg, C.; Schlaeppi, K.; Banerjee, S.; Kuramae, E.E.; van der Heijden, M.G. Fungal-bacterial diversity and microbiome complexity predict ecosystem functioning. *Nat. Commun.* **2019**, *10*, 4841. [CrossRef] [PubMed]
46. de Vries, F.T.; Griffiths, R.I.; Bailey, M.; Craig, H.; Girlanda, M.; Gweon, H.S.; Hallin, S.; Kaisermann, A.; Keith, A.M.; Kretzschmar, M.; et al. Soil bacterial networks are less stable under drought than fungal networks. *Nat. Commun.* **2018**, *9*, 3033. [CrossRef] [PubMed]
47. Chase, J.M. Stochastic community assembly causes higher biodiversity in more productive environments. *Science* **2010**, *328*, 1388–1391.
48. Graham, E.B.; Knelman, J.E. Implications of soil microbial community assembly for ecosystem restoration: Patterns, process, and potential. *Micro Ecol.* **2023**, *85*, 809–819. [CrossRef] [PubMed]
49. Zhou, J.; Ning, D. Stochastic community assembly: Does it matter in microbial ecology? *Microbiol. Mol. Biol. R.* **2017**, *81*, 10–1128. [CrossRef] [PubMed]
50. Menéndez-Serra, M.; Ontiveros, V.J.; Cáliz, J.; Alonso, D.; Casamayor, E.O. Understanding stochastic and deterministic assembly processes in microbial communities along temporal, spatial and environmental scales. *Mol. Ecol.* **2023**, *32*, 1629–1638. [CrossRef] [PubMed]
51. Xu, J.; Chen, Y.; Zhang, L.; Chai, Y.; Wang, M.; Guo, Y.; Li, T.; Yue, M. Using phylogeny and functional traits for assessing community assembly along environmental gradients: A deterministic process driven by elevation. *Ecol. Evol.* **2017**, *7*, 5056–5069. [CrossRef] [PubMed]
52. Levy-Booth, D.J.; Prescott, C.E.; Grayston, S.J. Microbial functional genes involved in nitrogen fixation, nitrification and denitrification in forest ecosystems. *Soil. Biol. Biochem.* **2014**, *75*, 11–25. [CrossRef]
53. Richardson, A.E.; Simpson, R.J. Soil microorganisms mediating phosphorus availability update on microbial phosphorus. *Plant Physiol.* **2011**, *156*, 989–996. [CrossRef]
54. Kuypers, M.M.; Marchant, H.K.; Kartal, B. The microbial nitrogen-cycling network. *Nat. Rev. Microbiol.* **2018**, *16*, 263–276. [CrossRef] [PubMed]

55. Glassman, S.I.; Wang, I.J.; Bruns, T.D. Environmental filtering by pH and soil nutrients drives community assembly in fungi at fine spatial scales. *Mol. Ecol.* **2017**, *26*, 6960–6973. [CrossRef] [PubMed]
56. Bahram, M.; Hildebrand, F.; Forslund, S.K.; Anderson, J.L.; Soudzilovskaia, N.A.; Bodegom, P.M.; Bengtsson-Palme, J.; Anslan, S.; Coelho, L.P.; Harend, H.; et al. Structure and function of the global topsoil microbiome. *Nature* **2018**, *560*, 233–237. [CrossRef] [PubMed]
57. Zhalnina, K.; Louie, K.B.; Hao, Z.; Mansoori, N.; da Rocha, U.N.; Shi, S.; Cho, H.; Karaoz, U.; Loqué, D.; Bowen, B.P.; et al. Dynamic root exudate chemistry and microbial substrate preferences drive patterns in rhizosphere microbial community assembly. *Nat. Microbiol.* **2018**, *3*, 470–480. [CrossRef] [PubMed]
58. Sardans, J.; Lambers, H.; Preece, C.; Alrefaei, A.F.; Penuelas, J. Role of mycorrhizas and root exudates in plant uptake of soil nutrients (calcium, iron, magnesium, and potassium): Has the puzzle been completely solved? *Plant J.* **2023**, *114*, 1227–1242. [CrossRef]
59. Steinauer, K.; Thakur, M.P.; Emilia Hannula, S.; Weinhold, A.; Uthe, H.; van Dam, N.M.; Martijn Bezemer, T. Root exudates and rhizosphere microbiomes jointly determine temporal shifts in plant-soil feedbacks. *Plant Cell Env.* **2023**, *46*, 1885–1899. [CrossRef] [PubMed]
60. Kivlin, S.N.; Winston, G.C.; Goulden, M.L.; Treseder, K.K. Environmental filtering affects soil fungal community composition more than dispersal limitation at regional scales. *Fungal Ecol.* **2014**, *12*, 14–25. [CrossRef]
61. Lareen, A.; Burton, F.; Schäfer, P. Plant root-microbe communication in shaping root microbiomes. *Plant Mol. Biol.* **2016**, *90*, 575–587. [CrossRef]
62. Kang, E.; Li, Y.; Zhang, X.; Yan, Z.; Wu, H.; Li, M.; Yan, L.; Wang, J.; Kang, X. Soil pH and nutrients shape the vertical distribution of microbial communities in an alpine wetland. *Sci. Total Environ.* **2021**, *774*, 145780. [CrossRef]